R. & M. No. 3429

MINISTRY OF AVIATION

AERONAUTICAL RESEARCH COUNCIL
REPORTS AND MEMORANDA

Torsional Flutter of Unstalled Cascade Blades at Zero Deflection

By D. S. WHITEHEAD, M.A., Ph.D., A.M.I.Mech.E., A.F.R.Ae.S.
CAMBRIDGE UNIVERSITY ENGINEERING LABORATORY

LONDON: HER MAJESTY'S STATIONERY OFFICE
1966
PRICE 9*s*. 6*d*. NET

Torsional Flutter of Unstalled Cascade Blades at Zero Deflection

By D. S. WHITEHEAD, M.A., Ph.D., A.M.I.Mech.E., A.F.R.Ae.S.
CAMBRIDGE UNIVERSITY ENGINEERING LABORATORY

*Reports and Memoranda No. 3429**
March, 1964

Summary.

The report presents the results of theoretical calculations of torsional flutter of unstalled cascade blades. It is shown that the position of the torsional axis is of great importance, the best position being near the quarter-chord point, and the worst position near the threequarter-chord point. An unfavourable axis position gives flutter speeds which are exceeded in normal machines.

An experimental investigation in an annular cascade with twelve blades confirms the existence of this type of flutter. Good agreement with the theory is found in some cases, but in others it is thought that three-dimensional effects are having a substantial influence.

The effects of small differences between blades are examined theoretically in an Appendix, and it is concluded that the effects of mistuning and mechanical damping are always favourable.

1. *Introduction.*

It has been well established that for normal designs of axial compressor and turbine blading the aerodynamic forces do not have an appreciable effect on the modes of vibration of the blades. This is because the mass of the blade is much greater than the mass of fluid in its immediate vicinity. In flutter investigations it is therefore sufficient to consider only a single degree of freedom in the motion of each blade, and this report will be concerned purely with torsional motion of each section about a known axis.

In an earlier theoretical investigation[1] of flutter of unstalled cascade blades at zero deflection it was found that whereas bending vibration was always damped, torsional vibration could be self-excited. These calculations were done using a method of dubious accuracy. In Ref. 2 an accurate method of calculation was presented, together with tables of force and moment coefficients. In the present report this more accurate method of calculation will be applied to the problem of torsional flutter, and an experimental study of the problem will also be described.

2. *Theory for Identical Blades.*

In the theory of Ref. 2 the assumptions are that the system is two-dimensional, that the fluid is incompressible and inviscid, that the blades are flat plates operating at zero mean incidence and that the blades do not stall. It is also assumed that the blades vibrate, all having the same small amplitude, and with a constant phase angle (β) between one blade and the next.

* Replaces A.R.C. 26 085.

The aerodynamic force ($Fe^{i\omega t}$) and moment about the leading edge ($M_0 e^{i\omega t}$) for each unit length of blade are then expressed in terms of force and moment coefficients as follows:

$$F = \pi\rho Uc(qC_{Fq} + \alpha U C_{F\alpha}), \tag{1}$$

$$M_0 = \pi\rho Uc^2(qC_{Mq} + \alpha U C_{M\alpha}). \tag{2}$$

In these expressions, $qe^{i\omega t}$ is the velocity of the leading edge of the blade due to its vibration and $\alpha e^{i\omega t}$ is the angular displacement of the blade. The notation is illustrated in Fig. 1.

If the blades vibrate in torsion about an axis distant ηc from the leading edge, then the moment about this axis $M_\eta e^{i\omega t}$ can be expressed in terms of a moment coefficient $(C_{M\alpha})_\eta$ as follows:

$$M_\eta = \pi\rho U^2 c^2 \alpha (C_{M\alpha})_\eta. \tag{3}$$

It is shown in Ref. 2 that this coefficient is related to the coefficients for the axis position at the leading edge as follows:

$$(C_{M\alpha})_\eta = C_{M\alpha} - \eta C_{F\alpha} - i\lambda\eta C_{Mq} + i\lambda\eta^2 C_{Fq}, \tag{4}$$

where λ is the frequency parameter ($\lambda = \omega c/U$).

In order to find the conditions for self-excited vibration or flutter of the system, these aerodynamic forces must be equated to the mechanical forces. It is assumed that all the blades are identical, that there is no mechanical coupling through the blade roots, and that only torsional motion about an axis position given by η is to be considered. Then the equation of motion for unit length of blade is

$$k\frac{d^2}{dt^2}(\alpha e^{i\omega t}) + \frac{k\omega_0\delta}{\pi}\frac{d}{dt}(\alpha e^{i\omega t}) + k\omega_0^2(\alpha e^{i\omega t}) = M_\eta e^{i\omega t},$$

where k = moment of inertia per unit length of blade,

ω_0 = natural frequency of blade in a vacuum,

δ = logarithmic decrement due to mechanical damping.

Using equation (3) this gives

$$k\left(-\omega^2 + \frac{i\omega\omega_0\delta}{\pi} + \omega_0^2\right) = \pi\rho U^2 c^2 (C_{M\alpha})_\eta. \tag{5}$$

It is convenient to define a non-dimensional moment of inertia parameter χ' as follows:

$$\chi' = k/\pi\rho c^4. \tag{6}$$

χ' represents the ratio of the moment of inertia of unit length of blade to the moment of inertia of a cylinder of air with diameter comparable to the blade chord. It is generally rather a large number.

For steady vibration both the real and imaginary parts of equation (5) must be satisfied. The real part gives

$$\chi'\lambda^2\frac{\omega_0^2 - \omega^2}{\omega^2} = \mathscr{R}(C_{M\alpha})_\eta. \tag{7}$$

The imaginary part gives

$$\chi'\lambda^2\frac{\omega_0}{\omega}\frac{\delta}{\pi} = \mathscr{I}(C_{M\alpha})_\eta. \tag{8}$$

Equation (7) gives the frequency at which flutter can occur. Since χ' is large, $(\omega_0^2 - \omega^2)$ is small and ω is nearly equal to ω_0.

Equation (8) relates the mechanical and aerodynamic damping, and is the condition for the flutter to be just self excited. Flutter can only occur if the imaginary part of $(C_{M\alpha})_\eta$ is positive, and then equation (8) can be regarded as giving the amount of mechanical damping required to just stop the flutter.

If there is no mechanical damping, then the condition for marginal flutter is

$$\mathscr{I}(C_{M\alpha})_\eta = 0,$$

or, from equation (4),

$$\mathscr{I}(C_{M\alpha}) - \eta\mathscr{I}(C_{F\alpha}) - \lambda\eta\mathscr{R}(C_{Mq}) + \lambda\eta^2\mathscr{R}(C_{Fq}) = 0. \tag{9}$$

Now these force and moment coefficients depend on four variables. These are the space to chord ratio (s/c), the stagger angle (ξ), the frequency parameter (λ), and the phasing angle (β). Since the calculation of the coefficients from the four numbers is rather long, it is convenient to regard equation (9) as a quadratic equation for the unknown axis position η, and it may have two roots, η_1, and η_2. These roots are shown plotted against β for a typical case in Fig. 2. It is seen that the lines of constant λ form loops, and inside these loops the imaginary part of $(C_{M\alpha})_\eta$ is positive and flutter can occur.

Now if there is a large number of blades in the cascade, flutter can occur at any value of the phase angle β. Taking the example shown in Fig. 2, this means that flutter will occur for any value of the axis position η between points A and B and also between points C and D. These are the critical values of η and a computer programme has been arranged to find them. It operates by hunting for maxima and minima in the graphs of η against β. It will be noted that there may also be non-significant maxima and minima, in this case at points E and F.

The results for the critical values of η are shown in Figs. 3, 4 and 5, which give the value of λ (which is in practice the dependent variable) plotted against η. The calculations have been done for space to chord ratios of 0·75, 1·0, and 1·5, and for various stagger angles. Flutter is predicted if the operating point is below the line drawn, that is if the frequency parameter is less than a critical value or if the flow velocity is greater than a critical value.

The corresponding phase angles are shown in Figs. 6, 7 and 8. The letters A, B, C, D, E and F are used to identify the corresponding branches on Figs. 3 to 5 and Figs. 6 to 8, and these letters also correspond to the maxima and minima shown on Fig. 2. Fig. 5 shows that for stagger angles of 60° and 75° the question of which is the significant maximum or minimum may change as the position of the torsional axis is varied. This gives rise to kinks in the curves of critical frequency parameter against axis position. In these diagrams most of the computed points relating to non-significant maxima and minima have been omitted.

In the limit $\lambda \to 0$ the critical phase angles are either 0 or π. The case $\beta = 0$ can be treated by actuator-disc methods[6], and the critical axis position is at the centre of pressure for steady potential flow.

3. *Experimental Investigation.*

3.1. *Design.*

Since the torsional flutter of unstalled blades predicted theoretically in the previous section had not been observed experimentally, except in the exploratory experiments carried out by Bellenot and d'Epinay[3], an experimental investigation of this effect was planned.

The flutter depends upon an interaction of one blade with the rest, and therefore an annular cascade with 12 test blades was chosen. The number of test blades was kept rather small in order to reduce the number of normal modes of the whole system and make the critical flutter mode easier to identify. A small number of blades also eases the manufacture and tuning problems, but it does mean that the three-dimensional effects may be substantial. Since the theory is two-dimensional the hub to tip diameter ratio was chosen as 0·8. Some of the leading dimensions for the experiment are therefore as follows:

Tip Radius	6·675 in.
Hub Radius	5·340 in.
Hub/Tip ratio	0·8
Mean Radius	6·0075 in.
Number of blades	12
Spacing at mean radius	3·145 in.
Blade chord	3·145 in.
Spacing/Chord ratio	1·0
Aspect ratio (Height/Chord)	0·425
Stagger angle	45°

A diagram of the annulus is shown in Fig. 9. In accordance with the assumptions in the theory, the test blades have zero camber and operate at zero incidence. There is therefore a row of 43 inlet guide vanes placed upstream of the test cascade, which were designed to give the required air inlet angle of 45°. A row of 94 outlet guide vanes downstream of the test cascade removes the whirl. There are axial gaps between these blade rows of just over two axial chords of the test cascade.

Fig. 10 shows the rig mounted on one of the two exits of a low-speed wind tunnel. The air enters the rig through a contraction (this is shown on Fig. 9, but is not visible in Fig. 10, as it is inside the large vessel on the left of the picture), and is exhausted to atmosphere through an annular diffuser.

Fig. 11 shows one of the test blades. These blades are untwisted, and have a lenticular profile (i.e. both surfaces of the blade are circular arcs), 10% thick. This profile was chosen for ease of manufacture and because Figs. 3 to 5 show that a symmetrical profile of this type with the torsional axis at the mid-point of the chord is susceptible to torsional flutter. This last consideration is of very little importance, because in this experiment the position of the torsional axis is determined entirely by the mounting, but it was felt that if the type of profile does have any aerodynamic effect, then this is the type of profile on which trouble may occur in practice.

The blade mounting is shown in Figs. 12 and 13. Each blade is carried by four spring-steel strips, arranged in the form of a cross. This mounting is comparatively flexible for torsional motion about an axis at the centre of the cross, but is rigid for all other types of motion. The frequency of torsional vibration could be varied by sliding the block to which the strips were clamped at their fixed end in a direction parallel to the axis. This alters the effective length of the strips, and therefore the stiffness of the mounting. The position of the torsional axis could also be varied by sliding the whole mounting in a direction parallel to the blade chord. The values of η available in this way are $-0{\cdot}048$, $0{\cdot}111$, $0{\cdot}270$, $0{\cdot}429$, $0{\cdot}588$, and $0{\cdot}748$.

Each blade is set up so that the gap between the flat surface on the outside of the casing and the corresponding surface on the hub of the blade is 0·005 in. Since this gap is in a plane normal to the axis of vibration, the width of the gap is not altered by the vibration.

The motion of the blades was observed by resistance strain gauges stuck onto the steel strips. Further instrumentation consisted of three static-pressure tappings on both the inside and outside walls of the annulus in planes upstream and downstream of the test cascade, and provision was made for traversing the airflow in these two planes by means of a three-hole yaw-meter.

3.2. *Development.*

During the initial running of the rig two main difficulties were encountered. The first difficulty was that when the rig was run with the torsional axis near the mid-chord point there was found to be a static deflection of the blades in the direction of increased stagger angle. This was sufficiently great to take up the clearance between the blades and the slots in the casing, so that no vibration could then be observed. Traversing showed that the mean flow angles both in front of and behind the cascade were very close to the design angles of 45°, but there was a substantial static-pressure drop across the cascade. This must be associated with an axial force on the blades, which presumably acts at a centre of pressure well forward of the mid-chord point. (For potential flow the centre of pressure is at 22% chord for this cascade.) This pressure drop can therefore account for the deflection observed. The trouble was cured by increasing the stagger of the inlet guide vanes by 3°, so that the mean flow angle at inlet to the test cascade was then 48°. This was found to neutralize the force on the blades and there was then no steady angular deflection of the blade due to the flow.

The rig was initially designed to be run on the suction side of the wind tunnel, with the idea of ensuring a smooth flow drawn straight from the atmosphere. The second main difficulty was that this arrangement was found to give a very unsteady flow. This was associated with a leakage flow inward through the 0·005 in. gap between the test blades and the casing, giving rise to separation in the corners of the cascade. The trouble was cured by transferring the rig to the outlet end of the wind tunnel, and inserting gauzes behind the outlet guide vanes until the static pressure on the outside wall of the casing was just above atmospheric. The flow through the gap between the blades and the casing is then outward, giving a small effect of boundary-layer suction in the corners of the cascade, and the steadiness of the flow was found to be much improved.

3.3. *Test Procedure.*

On each build of the rig the blades were tuned to have very nearly the same frequency in still air. This was done by inserting plugs into some of the spare holes tapped into the hub of the blade. These plugs can be seen in Fig. 12. It was possible by this means to get the frequencies the same to within ± 0·02 c/s on a basic frequency of about 25 c/s. The frequencies were measured by comparing the signal from a freely vibrating blade, with that from a decade oscillator, and observing any relative phase changes.

The mechanical damping of each blade was then measured by taking a photograph of a free vibration. A typical example is shown in Fig. 14. The logarithmic decrement, δ, was determined from the equation:

$$\delta = (1/N) \log_e (a_1/a_2).$$

where a_1 and a_2 are the initial and final amplitudes, and N is the number of cycles observed. In a typical build δ was found to vary from about 0·008 to 0·020 on different blades. This is a variation of nearly 3 to 1, although the actual values are reasonably small. Close examination of the records

shows that δ depends appreciably on the amplitude of vibration, but this effect has been neglected. It will be shown in the Appendix that it is permissible to take an arithmetic mean value of δ for all the blades in any build.

The air flow was then turned on and the motion of ten of the blades was observed on ten-channel strain-gauge equipment. As the airspeed is increased the vibration is at first small and of a random nature, but when the axis was toward the back of the blade it was found that the amplitude became large and was very nearly steady. This was recorded as the flutter point. A record from the ten-channel strain-gauge equipment is shown in Fig. 15. This equipment is only suitable for qualitative work, as the time scale is non-linear, and there is considerable interference between one channel and the rest. This is illustrated in Fig. 15 by the sixth line which is a dummy channel and should not show any vibration, but indicates an amplitude of nearly half that of the other ten channels. Nevertheless this photograph does show how the blades vibrate with similar amplitudes on each, and with a small phase change between one blade and the next.

In computing the results the air velocity was obtained from the difference between the reading of a total pressure probe in the upstream plane and the mean of the six wall static-pressure tappings in the downstream plane. This therefore gives a mean air velocity between the wakes in the downstream plane, and was thought to be the most representative velocity to use, since the flutter effect depends on the rate at which vorticity is carried downstream behind the cascade.

The values of χ' have been calculated from the stiffness of the spring mounting measured in a preliminary experiment and from the measured static frequencies. This enables the moment of inertia to be calculated, and hence χ'.

3.4. *Results and Comparison with Theory.*

The experimental results obtained are given in the 'Table of Results', and are compared with the theoretical expectations in Figs. 16 and 17.

These theoretical calculations differ from those in Section 2 in that only those axis positions which are available in the experiment have been considered, and also since there are 12 blades in the cascade the only allowable values of β are multiples of 30°, giving 12 possible values of β. Of these 12 values, the one which gives the greatest value of the imaginary part of $(C_{M\alpha})_\eta$ is the one which will give flutter. Fig. 16 shows the imaginary part of $(C_{M\alpha})_\eta$ plotted against λ for these values of β as full lines. Dotted lines refer to a value of β which does not give the maximum value of $\mathscr{I}(C_{M\alpha})_\eta$. The corresponding values of the real part of $(C_{M\alpha})_\eta$ are shown on Fig. 17. It may be noted that the restriction to 12 values of the phase angle has only a slight effect on the flutter condition with zero mechanical damping. For instance, for $\eta = 0{\cdot}588$ Fig. 16 indicates that the flutter condition for zero mechanical damping $\{\mathscr{I}(C_{M\alpha})_\eta = 0\}$ is at $\lambda = 1{\cdot}025$, with $\beta = 60°$, whereas Fig. 4 gives $\lambda = 1{\cdot}08$ with unrestricted phase angles. Fig. 7 shows that the corresponding critical phase angle is at $\beta/2\pi = 0{\cdot}125$, or $\beta = 45°$, so that this indicates the maximum possible effect due to restriction of phase angle.

The real and imaginary parts of the moment coefficient have been calculated from the experimental results using equations (7) and (8) and are also shown on Figs. 16 and 17.

For $\eta = 0{\cdot}588$ there are experimental points for three different frequencies. These three points agree well with each other, and with the theoretical results. The theoretical calculations show that the most critical phase angle should be $\beta = 60°$, whereas in fact flutter was observed with $\beta = 30°$. The theoretical line for $\beta = 30°$ is also shown dotted on Fig. 16 and is seen to be only slightly lower

than the $\beta = 60°$ line. Two of the experimental points lie almost exactly on the $\beta = 30°$ line, whereas the third is nearer the $\beta = 60°$ line. Fig. 17 shows that the flutter frequencies agree quite well with the $\beta = 30°$ theoretical prediction. It is interesting to note that even the quite small amount of mechanical damping present drops the critical frequency parameter from just over 1 to about 0·6.

With the axis position at $\eta = 0{\cdot}429$ flutter was again observed, but at a frequency parameter considerably lower than that predicted by theory, as indicated on Fig. 16. The experimental phase angle of $\beta = 60°$ agrees with the theory and Fig. 17 shows that the flutter frequency also agrees very well.

With the axis position at $\eta = 0{\cdot}748$, flutter was again observed, but the mode was such that the blades on one side of the rig were vibrating with large amplitude, whereas the amplitude of the blades on the other side of the rig was comparatively small. This made the determination of the mean phase angle uncertain. Fig. 16 shows that the critical frequency parameter was considerably below the theoretical prediction, but Fig. 17 shows that agreement on the flutter frequency is good. It is interesting to note that according to the theory the $\beta = 30°$ and $\beta = 60°$ modes are almost equally critical in this case, and in fact there is a changeover at $\lambda = 0{\cdot}6$.

With the torsional axis at positions given by $\eta = 0{\cdot}270$, $0{\cdot}111$, and $-0{\cdot}048$ no steady flutter could be observed. The airspeed was increased until the amplitude of the random vibration was large enough for some of the blades to hit the sides of the slots in the casing. These points are plotted on Fig. 16, and it will be observed that in each case the theoretical flutter velocity was exceeded. No measurements of phase angle or of frequency, accurate enough to enable the real part of the moment coefficient to be calculated, could be made.

A further interesting observation was made when the tunnel was run at an air velocity just below that required to give flutter. If one of the blades was set vibrating it was found that although this blade decayed fairly quickly, the vibration was passed onto one of its neighbours, and then onto the next blade, and could in fact be followed about half way round the rig. The motion therefore takes the form of a wave of vibration which decays as it moves round the rig. As the airspeed is increased the wave decays less rapidly, and when the flutter speed is reached the cascade is in continuous vibration. The motion can then be stopped by holding any one of the blades, so that the wave cannot progress round the annulus. The direction of motion of the wave is upwards and to the right along the cascade as drawn in Fig. 1. This is consistent with the idea that the wake of each blade excites the motion of the blade nearest to it.

4. *Conclusions.*

The principal conclusion is that torsional flutter of unstalled blades can occur if the flow velocity exceeds a certain critical velocity given by Figs. 3, 4 and 5. The position of the torsional axis is shown to be of great importance. The optimum position for the axis is near the centre of pressure for steady potential flow, that is at about 25% chord for widely spaced blades and further forward as the spacing is reduced. The worst place for the axis is at about 75% chord. The flutter requires a phase difference between adjacent blades, and if the blades were made to move in phase, for instance by connecting the tips together by a pair of lacing wires, then this type of flutter would be prevented.

It is interesting to compare these results with criteria that have been given for torsional flutter of stalled blades. Shannon[4] concludes that the average value of the frequency parameter at which stalled flutter starts is 1·5, whereas Armstrong and Stevenson[5] give a value of 1·6.

The experimental work confirms the existence of this type of flutter. Agreement with theory, after making an allowance for the average mechanical damping, was good when the axis position was at 58·8% chord, but at the two neighbouring axis positions the experimental airspeed for flutter exceeded the theoretical airspeed, and at the three most forward axis positions only random vibration could be observed.

It was thought that these discrepancies might be due to the small differences in mechanical damping and natural frequency between the blades, and this is examined theoretically in the Appendix. It is concluded that these effects have no appreciable effect on the stability of the system, although they do affect the relative amplitude and phase of the blades in the flutter mode. This applies to blades tuned to the same frequency to within about $\pm$ 0·2%. If the blades are not tuned accurately there is likely to be a considerable stabilizing effect. In a preliminary experiment it was found that the critical frequency parameter was 0·38 with blade frequencies within $\pm$ 3·0%, and this rose to 0·57 with the blades tuned to $\pm$ 0·3%.

It is thought that the discrepancies between theory and experiment must be due either to three-dimensional effects or to the presence of outlet guide vanes about two axial chords downstream of the trailing edge of the test cascade. Since there are only 12 blades in the cascade, and the hub/tip ratio is 0·8, the system is not very two-dimensional. The discrepancies occur at the lower values of the frequency parameter, which is where the wave length of the disturbances in the wakes of the blades is greatest, and so where these geometrical effects might be expected to have greatest influence.

The type of flutter discussed here may well be of importance for transonic compressor blading, as this type of blading often has a nearly symmetrical section with the torsional axis near the mid-chord point. This flutter may also be of importance on shrouded turbine blades, if the effect of the shroud is to shift the torsional axis aft along the chord. In this case the trouble could be cured by altering the design of the shroud to shift the torsional axis further forward.

NOTATION

c		Blade chord
k		Moment of inertia of blade per unit length
p	$=$	$(\omega^2-\omega_0{}^2)/\omega_0{}^2$
$qe^{i\omega t}$		Velocity of leading edge of blade due to vibration
r, s		Integers
s		Spacing of blades
t		Time
y		Amplitude of 'aerodynamic mode'
C_{Fq}, $C_{F\alpha}$, C_{Mq}, $C_{M\alpha}$		Force and moment coefficients defined by equations (1) and (2)
C		Diagonal matrix of moment coefficients
E		Square matrix with elements exp $(2\pi irs/N)$
$Fe^{i\omega t}$		Force per unit length of blade
I		Unit matrix
$M_0e^{i\omega t}$		Moment per unit length of blade about leading edge
$M_\eta e^{i\omega t}$		Moment per unit length of blade about torsional axis
M		Diagonal matrix with elements $(\gamma_s+i\delta_s/\pi)$
N		Number of blades in cascade
U		Fluid velocity
X		Column matrix with elements α_s
Y		Column matrix with elements y_r
$\alpha e^{i\omega t}$		Angular displacement of blade
β		Phase angle between one blade and the next. (This is normally measured in radians, but is sometimes quoted in degrees)
γ		Deviation of blade stiffness from datum
δ		Logarithmic decrement of blade
ηc		Distance of torsional axis from leading edge
λ		Frequency parameter $(\lambda = \omega c/U)$
ξ		Stagger angle
ρ		Fluid density
χ'		Moment of inertia parameter $(\chi' = k/\pi\rho c^4)$
ω		Angular frequency of flutter
ω_0		Angular natural frequency of blade in vacuum
$\mathscr{R}$		Indicates real part of complex quantity
$\mathscr{I}$		Indicates imaginary part of complex quantity

REFERENCES

No.	*Author(s)*	*Title, etc.*
1	D. S. Whitehead	The aerodynamics of axial compressor and turbine blade vibration. Cambridge University Ph.D. thesis. 1957.
2	D. S. Whitehead	Force and moment coefficients for vibrating aerofoils in cascade. A.R.C. R. & M. 3254. February, 1960.
3	C. Bellenot and J. L. d'Epinay ..	Self induced vibrations of turbomachine blades. Brown Boveri Review, Vol. 37, p. 368. 1950.
4	J. F. Shannon	Vibration problems in gas turbines, centrifugal and axial flow compressors. A.R.C. R. & M. 2226. March, 1945.
5	E. K. Armstrong and R. E. Stevenson	Some practical aspects of compressor blade vibration. *J. R. Ae. S.*, Vol. 64, p. 117. 1960.
6	D. S. Whitehead	The vibration of cascade blades treated by actuator disc methods. *Proc. I. Mech. E.*, Vol. 173, p. 555. 1959.

APPENDIX

The Effect of Small Differences Between Blades

General Theory.

An annular cascade of N blades will be considered. These blades differ slightly in their natural frequencies and in the mechanical damping of each of them, and it will be supposed that the differences in natural frequency arise from small differences in the elastic spring force, the inertia force being the same.

If conditions are such that the cascade is capable of steady torsional oscillation, then the angular deflection of the sth blade will be

$$\alpha_s e^{i\omega t}.$$

This is a marginal flutter condition.

The moment of the mechanical force about the torsional axis for the sth blade is then given by

$$-k\left\{\frac{d^2}{dt^2}(\alpha_s e^{i\omega t}) + \frac{\omega_0 \delta_s}{\pi}\frac{d}{dt}(\alpha_s e^{i\omega t}) + \omega_0{}^2(1+\gamma_s)\alpha_s e^{i\omega t}\right\}$$

where δ_s is the logarithmic decrement of the blade, and γ_s represents the small change in stiffness from a datum stiffness.

If

$$p = \frac{\omega^2 - \omega_0{}^2}{\omega_0{}^2}, \tag{A1}$$

representing the small difference between the datum frequency ω_0 and the flutter frequency ω, then the moment of the mechanical force can be written

$$-k\omega_0{}^2\{\gamma_s + (i\delta_s/\pi) - p\}\alpha_s e^{i\omega t},$$

where the difference between ω and ω_0 has been neglected in the γ and δ terms.

If X is a column matrix of all the values of α_s for $0 \leqslant s \leqslant (N-1)$, and M is a diagonal matrix, the elements in the main diagonal being the corresponding values of $(\gamma_s + i\delta_s/\pi)$, then the column matrix of the moments of the mechanical forces is given by

$$-k\omega_0{}^2\{M - pI\}Xe^{i\omega t}, \tag{A2}$$

where I is the unit matrix.

It is next necessary to express the moments of the aerodynamic forces in the same form. In Ref. 2 the aerodynamic forces and moments are calculated for 'aerodynamic modes' in which all blades have the same amplitude, and with a constant phase angle between one blade and the next. If the amplitude of the rth 'aerodynamic mode' is $y_r\{0 \leqslant r \leqslant (N-1)\}$, the corresponding amplitude of the sth blade is

$$\alpha_s = y_r e^{2\pi i r s/N},$$

since the phase angle between one blade and the next is $2\pi r/N$.

The flutter mode will in general contain components of all the 'aerodynamic modes'. The amplitude of the sth blade can therefore be written

$$\alpha_s = \sum_{r=0}^{N-1} y_r e^{2\pi i r s/N}.$$

This can be written in matrix form

$$X = EY, \tag{A3}$$

where Y is a column matrix of all the values of y_r, and E is a square matrix with elements $\exp(2\pi irs/N)$ in the sth row and rth column.

Equation (A3) can be inverted to give

$$Y = E^{-1}X. \tag{A4}$$

The elements of E^{-1} are $(1/N)\exp(-2\pi irs/N)$.

Now due to the rth 'aerodynamic mode' the aerodynamic moment on the sth blade is

$$\pi\rho U^2c^2C_{M\alpha}(2\pi r/N)e^{2\pi irs/N}y_re^{i\omega t},$$

where $C_{M\alpha}(\beta)$ is the moment coefficient for a phase angle β, and is also a function of space to chord ratio, stagger angle, frequency parameter, and axis position.

If C is a diagonal matrix, the elements in the main diagonal being $C_{M\alpha}(2\pi r/N)$, then the aerodynamic moment due to all the 'aerodynamic modes' is

$$\begin{aligned}&\pi\rho U^2c^2ECYe^{i\omega t}\\ &= \pi\rho U^2c^2ECE^{-1}Xe^{i\omega t}.\end{aligned} \tag{A5}$$

For steady vibration the total moment must be zero.
Equations (A2) and (A5) then give

$$\{-k\omega_0^2(M-pI)+\pi\rho U^2c^2ECE^{-1}\}Xe^{i\omega t}=0,$$

or

$$\left\{\left(M-\frac{1}{\lambda^2\chi'}ECE^{-1}\right)-pI\right\}X=0. \tag{A6}$$

This equation shows that p is an eigenvalue and X is an eigenvector of the complex matrix $\{M-(1/\lambda^2\chi')ECE^{-1}\}$. For a marginal flutter condition the imaginary part of p must be zero and the real part gives the flutter frequency from equation (A1).

Now suppose that in an actual case the matrix $\{M-(1/\lambda^2\chi')ECE^{-1}\}$ has been calculated and its eigenvalues and eigenvectors found. It is likely that none of the imaginary parts of p are zero, so that steady vibration is not possible. But if the mechanical damping on every blade was increased by the same amount, so that the elements of the diagonal matrix M become $(\gamma_s+i\delta_s/\pi+i\epsilon)$, then the imaginary parts of p will all be increased by an amount ϵ. If the extra damping is made very large, then the imaginary parts of p will all be positive, and the system will certainly be stable. As ϵ is gradually reduced from this extreme, the imaginary parts of p will all drop, until one of them becomes zero and flutter is then possible. For stability the condition is that ϵ must be large enough to make all the imaginary parts of p positive. In the initial case the condition for the absence of flutter is that the imaginary parts of the eigenvalues of the matrix $\{M-(1/\lambda^2\chi')ECE^{-1}\}$ must all be positive.

A slightly different formulation in terms of the 'aerodynamic modes' is also possible. Equation (A6) can be written

$$\left\{\left(E^{-1}ME-\frac{1}{\lambda^2\chi'}C\right)-pI\right\}Y=0. \tag{A7}$$

This shows that p is also an eigenvalue of the matrix $\{E^{-1}ME-(1/\lambda^2\chi')C\}$, and the corresponding eigenvector is Y.

Bounds on the Eigenvalues.

It will be convenient to use the symbol ′ to denote a conjugate matrix and the symbol* to denote a transposed matrix.

Then from equation (A3):

$$X^{*\prime}X = Y^{*\prime}E^{*\prime}EY.$$

But E' has elements $\exp(-2\pi irs/N)$, so that

$$E^{*\prime} = NE^{-1}. \tag{A8}$$

Hence

$$X^{*\prime}X = NY^{*\prime}Y. \tag{A9}$$

Also from equation (A6) on premultiplying by $X^{*\prime}$:

$$X^{*\prime}MX - \frac{1}{\lambda^2\chi'} X^{*\prime}ECE^{-1}X - pX^{*\prime}X = 0.$$

Using equations (A4) and (A8) this can be written:

$$X^{*\prime}MX - \frac{N}{\lambda^2\chi'} Y^{*\prime}CY - pX^{*\prime}X = 0,$$

or, using equation (A9)

$$p = \frac{X^{*\prime}MX}{X^{*\prime}X} - \frac{1}{\lambda^2\chi'}\frac{Y^{*\prime}CY}{Y^{*\prime}Y}. \tag{A10}$$

Writing this in the form of summations

$$p = \frac{\sum_{s=0}^{N-1}\{|\alpha_s|^2(\gamma_s + i\delta_s/\pi)\}}{\sum_{s=0}^{N-1}|\alpha_s|^2} - \frac{1}{\lambda^2\chi'}\frac{\sum_{r=0}^{N-1}\{|y_r|^2 C_{M\alpha}(2\pi r/N)\}}{\sum_{r=0}^{N-1}|y_r|^2}. \tag{A11}$$

Consider the real part of this equation. If $(\gamma_s)_{\max}$ is the greatest of the values of γ_s, and $\mathscr{R}(C_{M\alpha})_{\min}$ is the least of the real parts of $C_{M\alpha}$, then

$$\mathscr{R}(p) < (\gamma_s)_{\max} - \frac{1}{\gamma^2\chi'}\mathscr{R}(C_{M\alpha})_{\min}. \tag{A12}$$

Similarly

$$\mathscr{R}(p) > (\gamma_s)_{\min} - \frac{1}{\lambda^2\chi'}\mathscr{R}(C_{M\alpha})_{\max}, \tag{A13}$$

$$\mathscr{I}(p) < \frac{1}{\pi}(\delta_s)_{\max} - \frac{1}{\lambda^2\chi'}\mathscr{I}(C_{M\alpha})_{\min}, \tag{A14}$$

and

$$\mathscr{I}(p) > \frac{1}{\pi}(\delta_s)_{\min} - \frac{1}{\lambda^2\chi'}\mathscr{I}(C_{M\alpha})_{\max}. \tag{A15}$$

Of these bounds to the eigenvalues, the most interesting is (A15). If all the imaginary parts of $C_{M\alpha}$ are negative, so that a system with identical blades cannot flutter, this shows that the imaginary parts of p are all positive, and the system is always stable. This proves that the effect of mechanical damping and mistuning of the blades is always stabilizing.

Approximations to the Eigenvalues.

Equation (A11) can sometimes be used as an extension of Rayleigh's Principle to obtain approximations to the eigenvalues. If the form of the eigenvector can be guessed then this equation will give an approximate value for p.

In particular, if the mechanical differences between the blades are very small, it may be supposed that the flutter mode will not differ much from an 'aerodynamic mode' in which $|\alpha_s|$ is the same for all blades, and all the values of y_r are zero except for one. Then equation (A11) gives

$$p = \frac{1}{N} \sum_{s=0}^{N-1} (\gamma_s + i\delta_s/\pi) - \frac{1}{\lambda^2 \chi'} C_{M\alpha}. \tag{A16}$$

This shows that the values of p correspond to the values of $C_{M\alpha}$, modified by the arithmetic mean of the mistuning and mechanical damping effects. It will be noted that spurious components of other 'aerodynamic modes' will have only a second-order effect.

Alternatively if the aerodynamic coupling between the blades is very weak, it may be guessed that the flutter modes will not differ much from the motion of single blades. All the values of α_s are zero except for one and $|y_r|$ is the same for all 'aerodynamic modes'. Then equation (A11) gives

$$p = (\gamma_s + i\delta_s/\pi) - \frac{1}{\lambda^2 \chi'} \frac{1}{N} \sum_{r=0}^{N-1} C_{M\alpha}(2\pi r/N). \tag{A17}$$

This shows that the mechanical properties of each blade are modified by an arithmetic mean of the aerodynamic coefficients. Again spurious components in the mode will have only a second-order effect.

Numerical Results.

The experiments reported in the main body of the report showed that in some cases flutter was not observed under conditions in which it should theoretically occur. It was thought that this might be due to the effects of residual mistuning and different amounts of mechanical damping on each blade. A computer programme was therefore written to evaluate the matrix $\{M - (1/\lambda^2\chi) ECE^{-1}\}$ and find its eigenvalues and eigenvectors. The method used to find the eigenvalues is a generalization of the Jacobi process for real symmetric matrices, and operates by successive iterations in which the matrix is gradually reduced to diagonal form, with the eigenvalues in the leading diagonal.

Some typical results are shown in Fig. 18, which shows the eigenvalues plotted on an Argand diagram as circled points. These are really twelve distinct points, but since they lie very nearly on a continuous loop a line has been drawn through them.

Also shown as triangles are the values of $(\gamma_s + i\delta_s/\pi)$, and these form a cluster just above the origin. These points are the eigenvalues of the diagonal matrix M, and represent the mechanical effects only.

The points shown as crosses are the values of $-(1/\lambda^2\chi') C_{M\alpha}(2\pi r/N)$ and these do lie accurately on a continuous loop. These points are the eigenvalues of the matrix $-(1/\lambda^2\chi') ECE^{-1}$ and represent the aerodynamic effects only.

It is seen that the combined effect can be obtained accurately from equation (A16); that is by shifting the curve for the aerodynamic effects bodily through a distance given by the arithmetic mean of the points for the mechanical effects only. This was true for all the cases computed, and the other results are therefore not presented here.

Fig. 18 shows that if aerodynamic effects only are included there are four points with negative imaginary parts, indicating instability. When the effects of mechanical damping and mistuning are included, there are still three points indicating instability. This is for a frequency parameter of 0·4, whereas it was found in the experiment that the frequency parameter had to be reduced to 0·335 for the flutter to appear. It is concluded that the effects of mistuning and differences in mechanical damping will not account for the discrepancy between theory and some of the experiments.

Fig. 19 shows the eigenvector corresponding to the least stable circled point on Fig. 18. This is the flutter mode associated with $r = 2$ ($\beta = 60°$). Fig. 19 shows that the phase angle between one blade and the next is approximately 60°, but that there is an appreciable variation of amplitude and phase angle on moving around the cascade. It is concluded from this and other cases that whereas the effect of small differences between blades on the stability of the system can be adequately accounted for by using a mean mechanical damping factor, these small differences do have an appreciable effect on the nature of the flutter mode.

It will be noted that although this Appendix has been written in terms of torsional vibration, exactly the same arguments apply to bending vibration, or to flutter in which two or more modes are aerodynamically coupled.

TABLE OF RESULTS

Axis Position η	− 0·048	0·111	0·270	0·429	0·588	0·588	0·588	0·748
Spring Length in.	1·5	2·0	2·0	2·0	3·0	2·0	1·5	1·5
Static Frequency ω_0 c/s	23·12	22·38	28·41	30·75	20·51	27·66	36·51	30·44
Mean δ	0·0154	0·0122	0·0116	0·0137	0·0128	0·0129	0·0158	0·0180
χ'	31·1	20·2	12·3	10·9	14·4	13·0	12·4	17·75
Air Velocity U ft/sec	211	262	274	144	57·3	76·4	92·5	140
Frequency Parameter λ	0·182	0·140	0·171	0·335	0·577	0·585	0·636	0·359
Comment	Random	Random	Random	Flutter	Flutter	Flutter	Flutter	Flutter
Flutter Frequency ω c/s	?	?	?	29·27	20·10	27·13	35·75	28·00
Mean $\beta°$	—	—	—	60°	30°	30°	30°	?
$\lambda^2\chi'\delta/\pi$	0·00250	0·00155	0·00133	0·00533	0·0195	0·0183	0·0252	0·0131
$\lambda^2\chi'(\omega_0^2-\omega^2)/\omega^2$	—	—	—	0·124	0·194	0·174	0·213	0·399

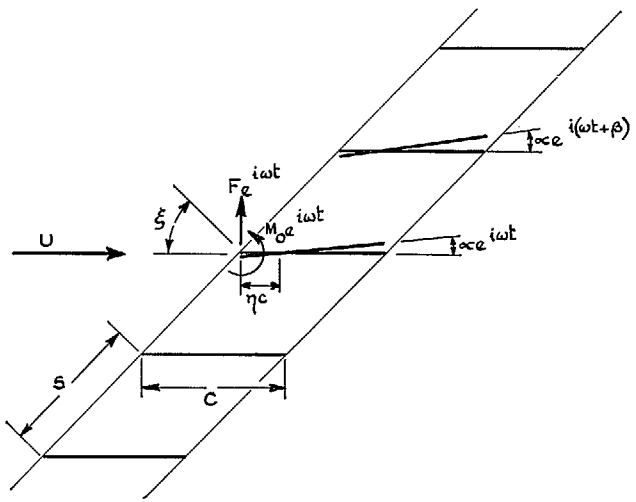

FIG. 1. Illustration of notation.

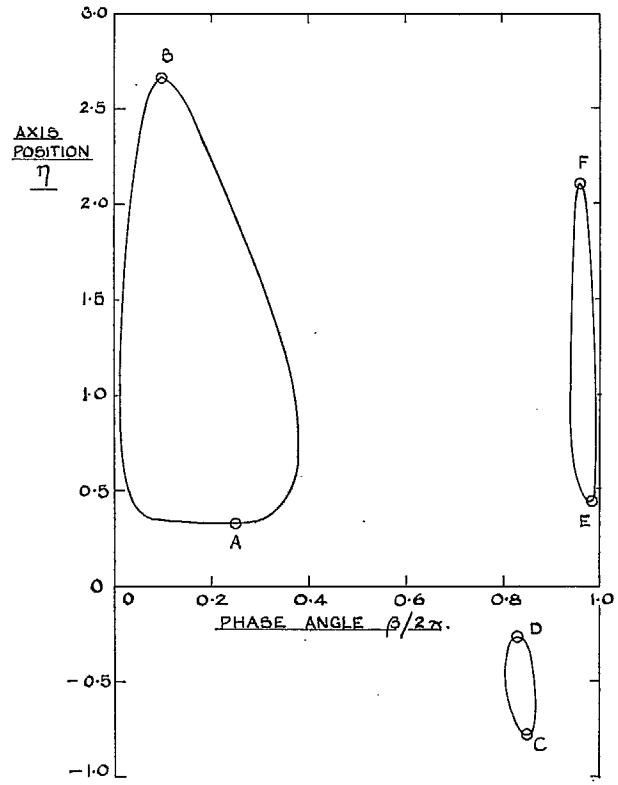

FIG. 2. Critical axis positions: $s/c = 1{\cdot}0$, $\xi = 75°$, $\lambda = 0{\cdot}5$.

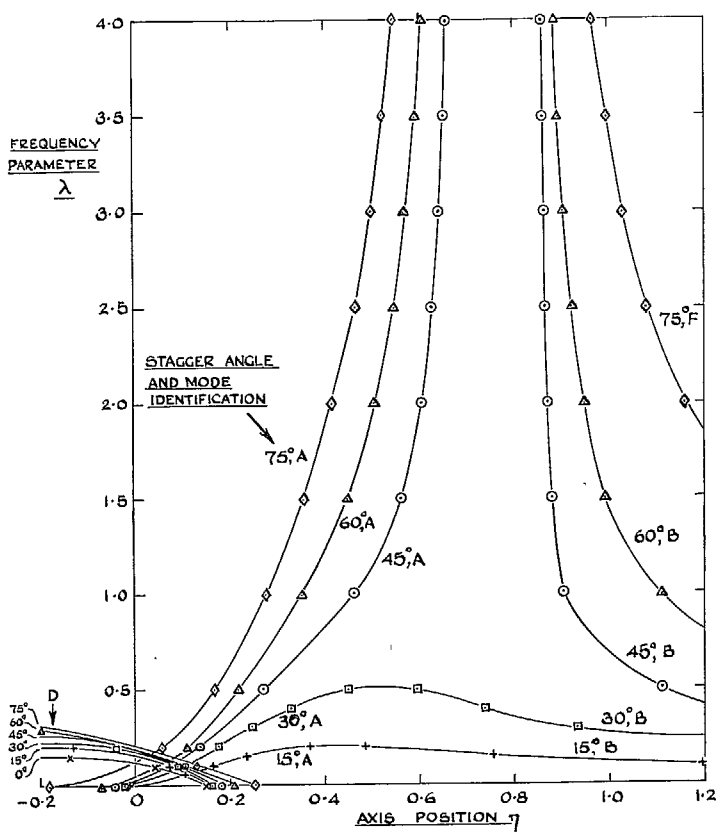

FIG. 3. Critical frequency parameter for flutter: $s/c = 0{\cdot}75$.

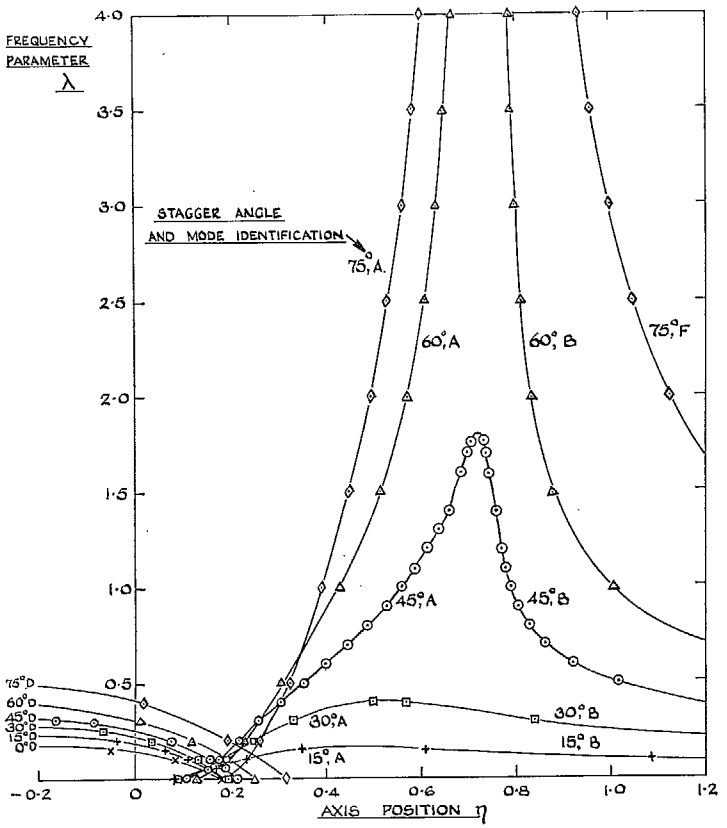

FIG. 4. Critical frequency parameter for flutter: $s/c = 1{\cdot}0$.

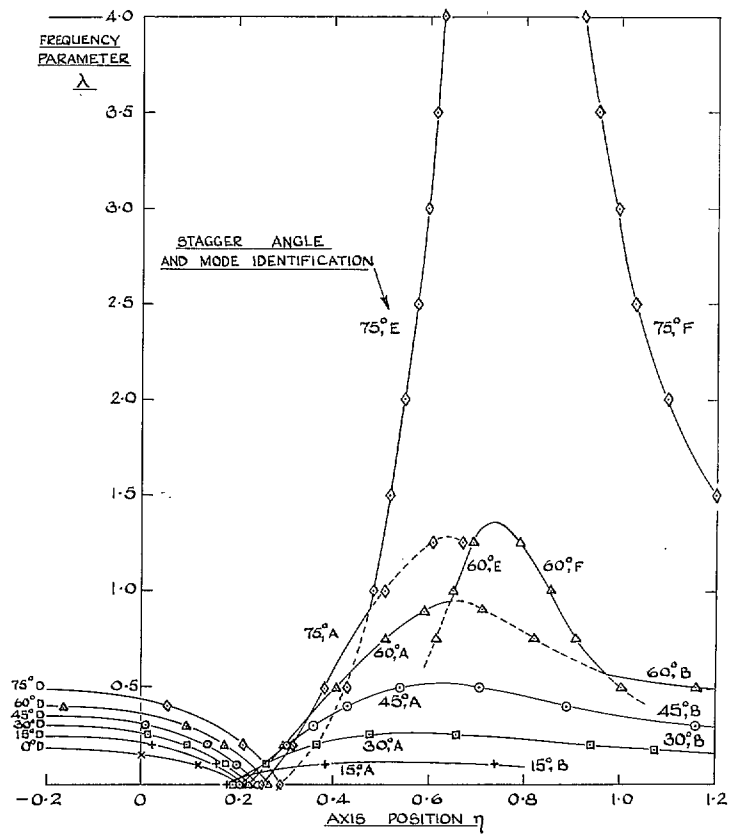

FIG. 5. Critical frequency parameter for flutter: $s/c = 1{\cdot}5$.

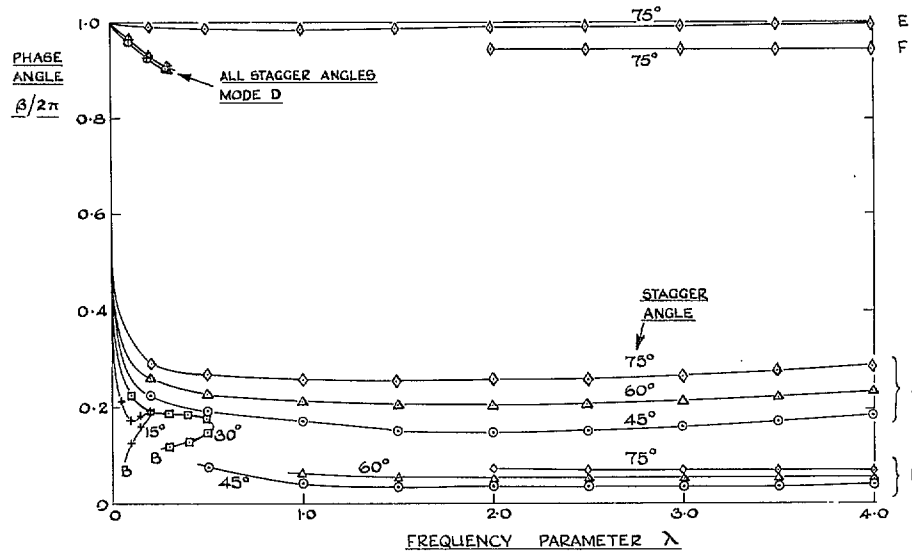

FIG. 6. Critical phase angles: $s/c = 0{\cdot}75$.

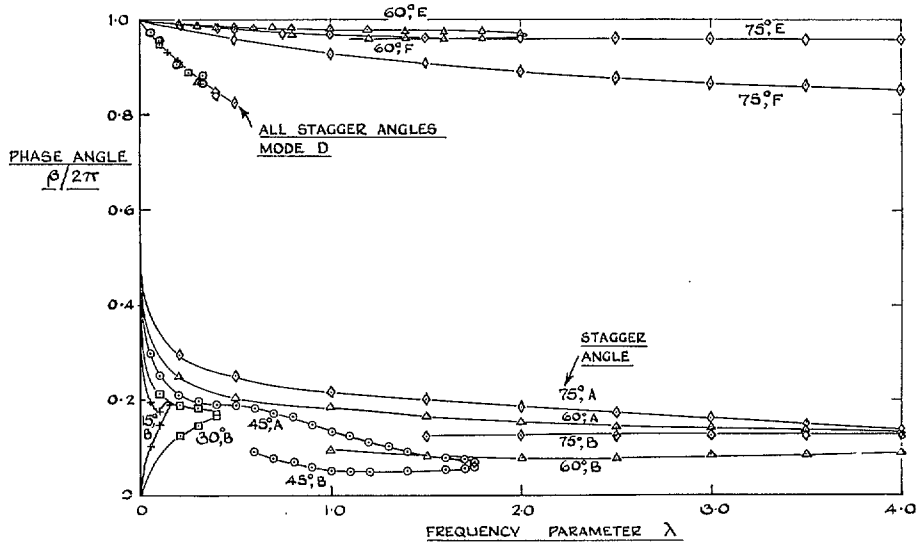

FIG. 7. Critical phase angles: $s/c = 1{\cdot}0$.

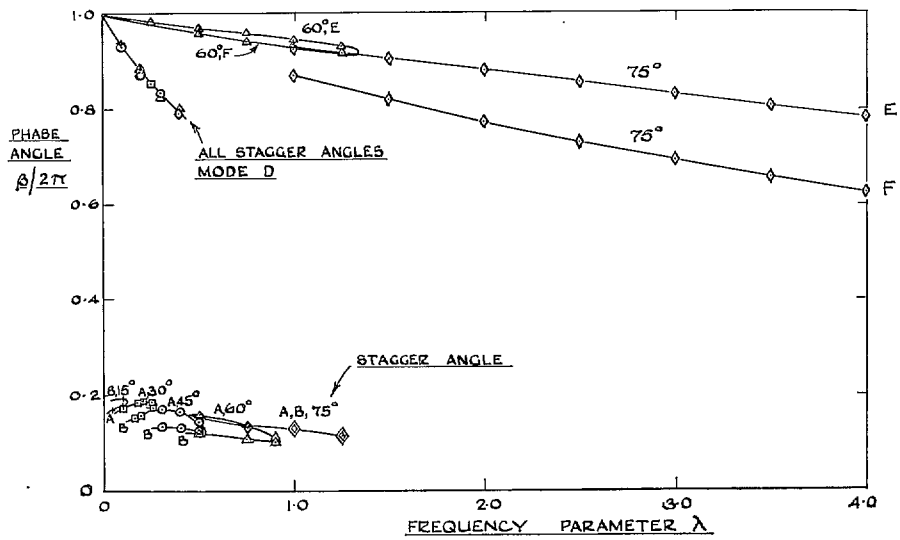

FIG. 8. Critical phase angles: $s/c = 1{\cdot}5$.

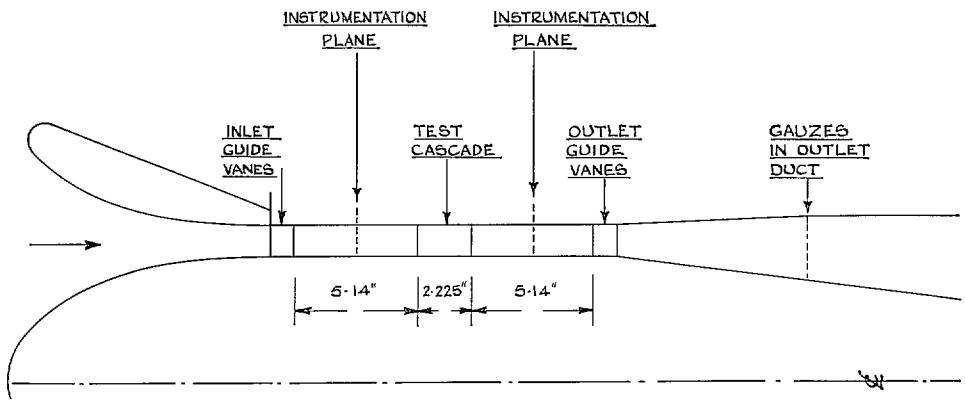

FIG. 9. Annulus diagram.

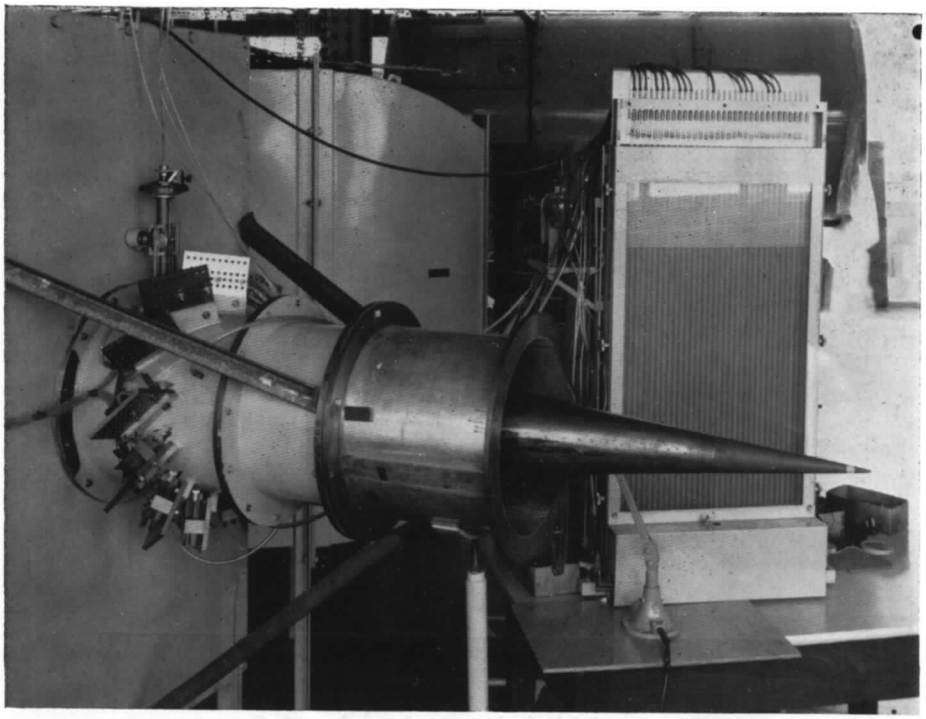

FIG. 10. General view of rig.

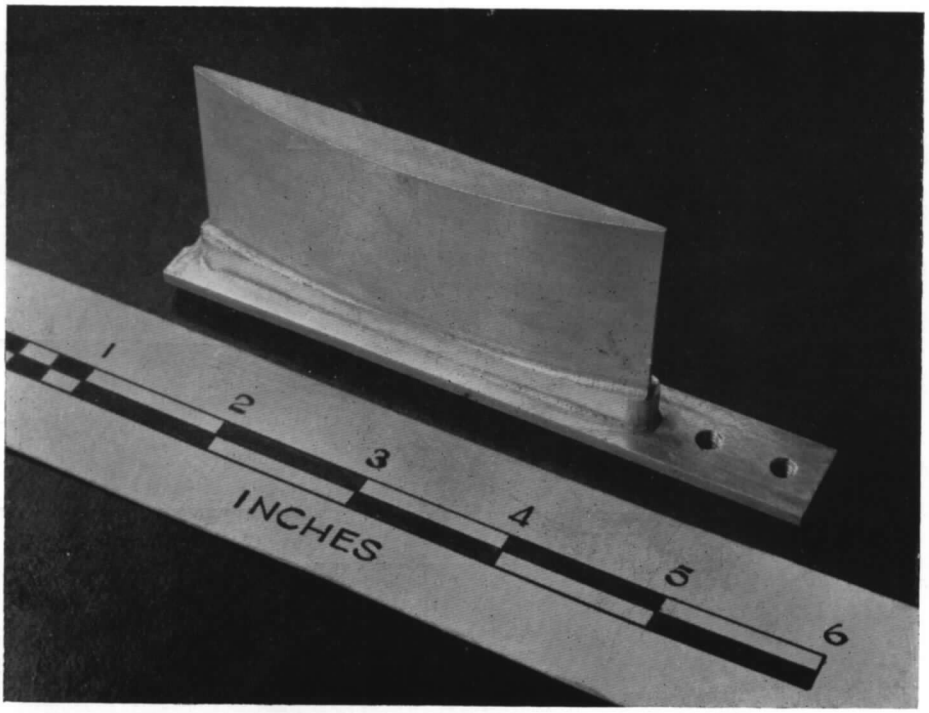

FIG. 11. Test blade.

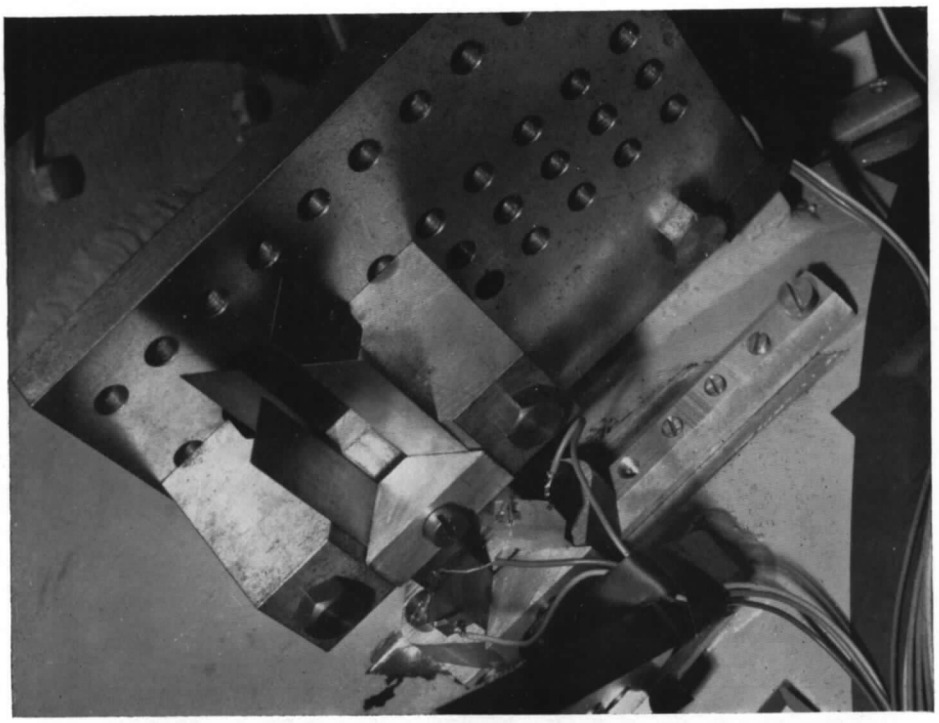

FIG. 12. Blade mounting.

FIG. 13. Blade mounting.

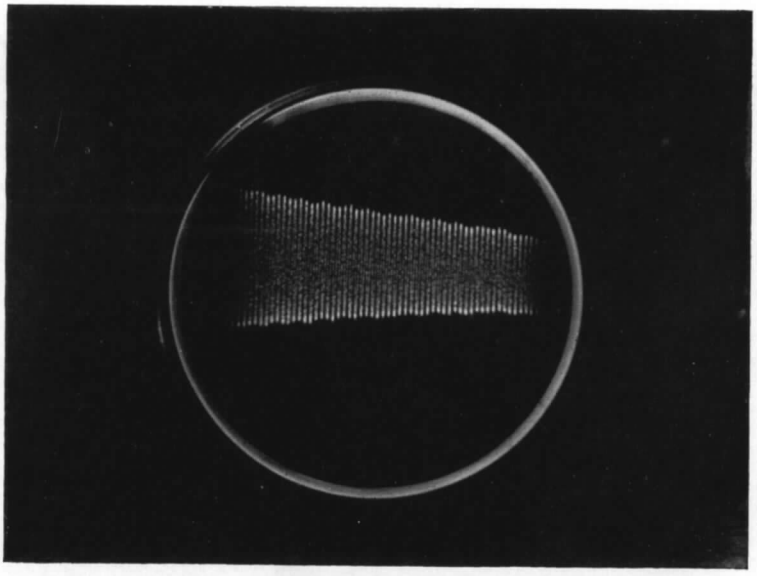

FIG. 14. Decay of vibration in still air ($\eta = 0{\cdot}27$, $f = 28{\cdot}4$ c/s, Blade No. 5, $\delta = 0{\cdot}012$).

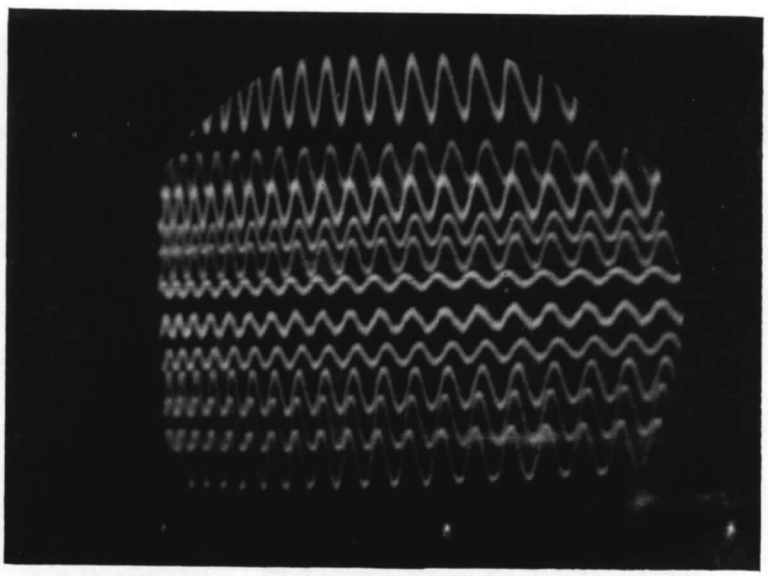

FIG. 15. Record of flutter point ($\eta = 0{\cdot}588$, $f = 27{\cdot}66$ c/s).

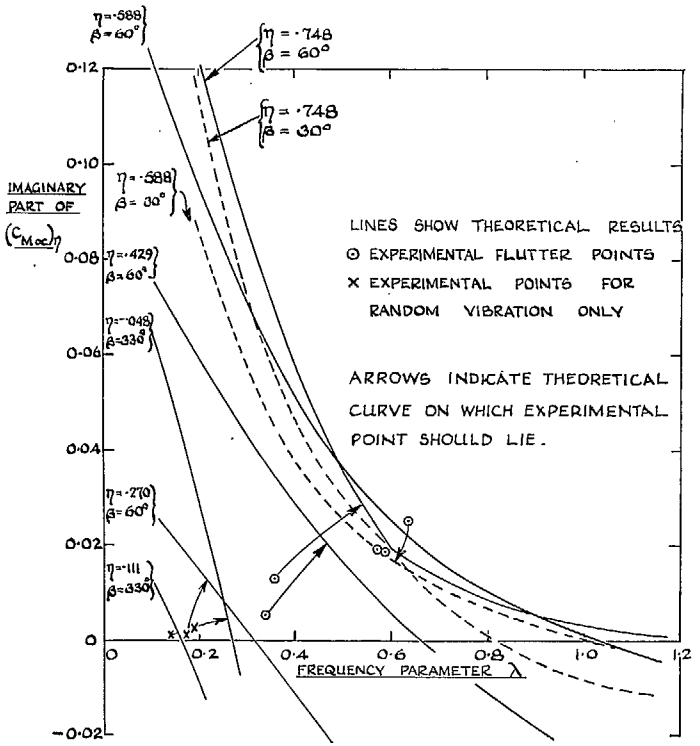

FIG. 16. Comparison with experiment: imaginary part of coefficient: $s/c = 1$, $\xi = 45°$.

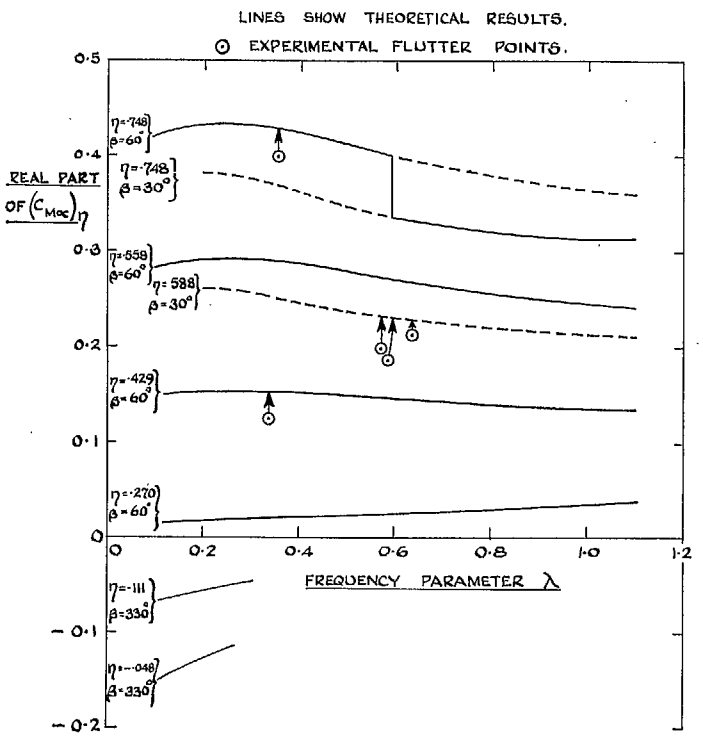

FIG. 17. Comparison with experiment: real part of coefficient: $s/c = 1$, $\xi = 45°$.

(92364) Wt. 67/7689 K.5 9/66 Hw.

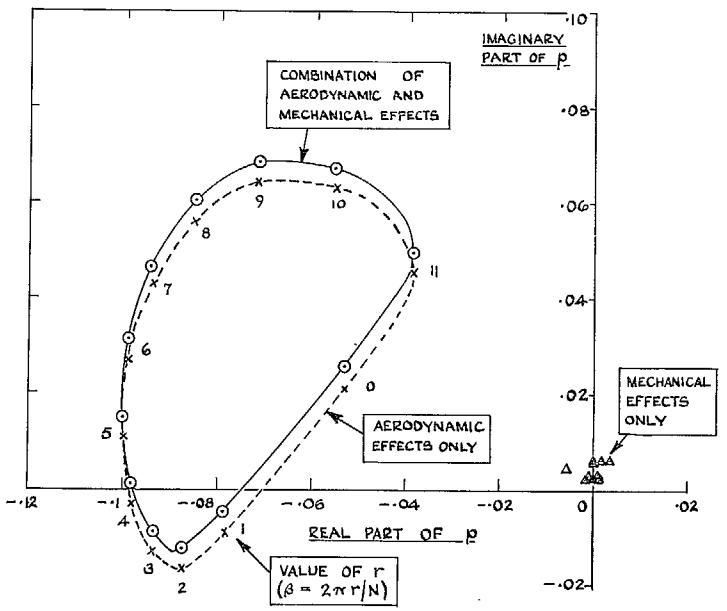

FIG. 18. Effect of small blade differences on eigenvalues: $s/c = 1$, $\xi = 45°$, $\lambda = 0{\cdot}4$, $\eta = 0{\cdot}429$, $\chi' = 10{\cdot}9$, $N = 12$.

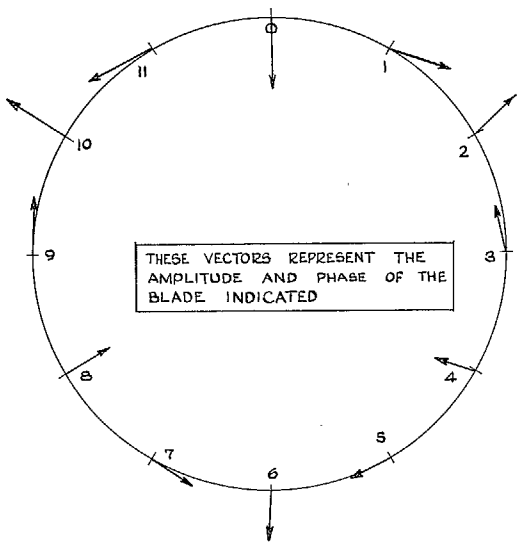

FIG. 19. Effect of small blade differences on eigenvector: $s/c = 1$, $\xi = 45°$, $\lambda = 0{\cdot}4$, $\eta = 0{\cdot}429$, $\chi = 10{\cdot}9$, $N = 12$.

Publications of the Aeronautical Research Council

ANNUAL TECHNICAL REPORTS OF THE AERONAUTICAL RESEARCH COUNCIL (BOUND VOLUMES)

1945 Vol. I. Aero and Hydrodynamics, Aerofoils. £6 10s. (£6 14s.)
Vol. II. Aircraft, Airscrews, Controls. £6 10s. (£6 14s.)
Vol. III. Flutter and Vibration, Instruments, Miscellaneous, Parachutes, Plates and Panels, Propulsion. £6 10s. (£6 14s.)
Vol. IV. Stability, Structures, Wind Tunnels, Wind Tunnel Technique. £6 10s. (£6 14s.)

1946 Vol. I. Accidents, Aerodynamics, Aerofoils and Hydrofoils. £8 8s. (£8 12s. 6d.)
Vol. II. Airscrews, Cabin Cooling, Chemical Hazards, Controls, Flames, Flutter, Helicopters, Instruments and Instrumentation, Interference, Jets, Miscellaneous, Parachutes. £8 8s. (£8 12s.)
Vol. III. Performance, Propulsion, Seaplanes, Stability, Structures, Wind Tunnels. £8 8s. (£8 12s.)

1947 Vol. I. Aerodynamics, Aerofoils, Aircraft. £8 8s. (£8 12s. 6d.)
Vol. II. Airscrews and Rotors, Controls, Flutter, Materials, Miscellaneous, Parachutes, Propulsion, Seaplanes, Stability, Structures, Take-off and Landing. £8 8s. (£8 12s. 6d.)

1948 Vol. I. Aerodynamics, Aerofoils, Aircraft, Airscrews, Controls, Flutter and Vibration, Helicopters, Instruments, Propulsion, Seaplane, Stability, Structures, Wind Tunnels. £6 10s. (£6 14s.)
Vol. II. Aerodynamics, Aerofoils, Aircraft, Airscrews, Controls, Flutter and Vibration, Helicopters, Instruments, Propulsion, Seaplane, Stability, Structures, Wind Tunnels. £5 10s. (£5 14s.)

1949 Vol. I. Aerodynamics, Aerofoils. £5 10s. (£5 14s.)
Vol. II. Aircraft, Controls, Flutter and Vibration, Helicopters, Instruments, Materials, Seaplanes, Structures, Wind Tunnels. £5 10s. (£5 13s. 6d.)

1950 Vol. I. Aerodynamics, Aerofoils, Aircraft. £5 12s. 6d. (£5 16s. 6d.)
Vol. II. Apparatus, Flutter and Vibration, Meteorology, Panels, Performance, Rotorcraft, Seaplanes. £4 (£4 3s. 6d.)
Vol. III. Stability and Control, Structures, Thermodynamics, Visual Aids, Wind Tunnels. £4 (£4 3s. 6d.)

1951 Vol. I. Aerodynamics, Aerofoils. £6 10s. (£6 14s.)
Vol. II. Compressors and Turbines, Flutter, Instruments, Mathematics, Ropes, Rotorcraft, Stability and Control, Structures, Wind Tunnels. £5 10s. (£5 14s.)

1952 Vol. I. Aerodynamics, Aerofoils. £8 8s. (£8 12s.)
Vol. II. Aircraft, Bodies, Compressors, Controls, Equipment, Flutter and Oscillation, Rotorcraft, Seaplanes, Structures. £5 10s. (£5 13s. 6d.)

1953 Vol. I. Aerodynamics, Aerofoils and Wings, Aircraft, Compressors and Turbines, Controls. £6 (£6 4s.)
Vol. II. Flutter and Oscillation, Gusts, Helicopters, Performance, Seaplanes, Stability, Structures, Thermodynamics, Turbulence. £5 5s. (£5 9s.)

1954 Aero and Hydrodynamics, Aerofoils, Arrester gear, Compressors and Turbines, Flutter, Materials, Performance, Rotorcraft, Stability and Control, Structures. £7 7s. (£7 11s.)

Special Volumes

Vol. I. Aero and Hydrodynamics, Aerofoils, Controls, Flutter, Kites, Parachutes, Performance, Propulsion, Stability. £6 6s. (£6 9s. 6d.)
Vol. II. Aero and Hydrodynamics, Aerofoils, Airscrews, Controls, Flutter, Materials, Miscellaneous, Parachutes, Propulsion, Stability, Structures. £7 7s. (£7 10s. 6d.)
Vol. III. Aero and Hydrodynamics, Aerofoils, Airscrews, Controls, Flutter, Kites, Miscellaneous, Parachutes, Propulsion, Seaplanes, Stability, Structures, Test Equipment. £9 9s. (£9 13s. 6d.)

Reviews of the Aeronautical Research Council

1949–54 5s. (5s. 6d.)

Index to all Reports and Memoranda published in the Annual Technical Reports

1909–1947 R. & M. 2600 (out of print)

Indexes to the Reports and Memoranda of the Aeronautical Research Council

Between Nos. 2451–2549: R. & M. No. 2550 2s. 6d. (2s. 9d.); Between Nos. 2651–2749: R. & M. No. 2750 2s. 6d. (2s. 9d.); Between Nos. 2751–2849: R. & M. No. 2850 2s. 6d. (2s. 9d.); Between Nos. 2851–2949: R. & M. No. 2950 3s. (3s. 3d.); Between Nos. 2951–3049: R. & M. No. 3050 3s. 6d. (3s. 9d.); Between Nos. 3051–3149: R. & M. No. 3150 3s. 6d. (3s. 9d.); Between Nos. 3151–3249: R. & M. No. 3250 3s. 6d. (3s. 9d.); Between Nos. 3251–3349: R. & M. No. 3350 3s. 6d. (3s. 11d.)

Prices in brackets include postage

Government publications can be purchased over the counter or by post from the Government Bookshops in London, Edinburgh, Cardiff, Belfast, Manchester, Birmingham and Bristol, or through any bookseller

Printed and published by
HER MAJESTY'S STATIONERY OFFICE

To be purchased from
49 High Holborn, London WC1
423 Oxford Street, London W1
13A Castle Street, Edinburgh 2
109 St. Mary Street, Cardiff
Brazennose Street, Manchester 2
50 Fairfax Street, Bristol 1
35 Smallbrook, Ringway, Birmingham 5
80 Chichester Street, Belfast 1
or through any bookseller

Printed in England

S.O. Code No. 23-3429